

Preparation of $\text{Sm}_2\text{Fe}_{17}\text{N}_x$ Powders and Their Bonded Magnets with High-Performance Permanent Magnetic Characteristics

Hirokazu Izumi, Ken-ichi Machida,* Atsushi Shiomi, Masayuki Iguchi, Kenji Noguchi, and Gin-ya Adachi*

Department of Applied Chemistry, Faculty of Engineering, Osaka University, 2-1 Yamadaoka, Suita, Osaka 565, Japan

Received January 13, 1997. Revised Manuscript Received August 28, 1997[®]

Uniformly ground $\text{Sm}_2\text{Fe}_{17}\text{N}_x$ fine powders with high-performance permanent magnetic property and oxidation resistance characteristics were obtained from the coarse powders by ball milling in an organic solution containing a surfactant and surface modification for them, followed by fabrication of their bonded magnets. Their remanence (B_r) and coercivity (H_{cj}) values were well-balanced and considerably higher than those for the samples prepared by conventional methods, and a huge maximum energy product $(\text{BH})_{\text{max}}$ around 330 kJ m^{-3} was consequently attained as a reproducible average. The $\text{Sm}_2\text{Fe}_{17}\text{N}_x$ powder stabilized by surface coating with the zinc metal produced via photodecomposition of diethylzinc ($\text{Zn}(\text{C}_2\text{H}_5)_2$) showed the better oxidation resistivity than the uncoated samples, so that the B_r , H_{cj} , and $(\text{BH})_{\text{max}}$ values were maintained at high levels even after the heat treatment at 353–423 K for several hours as required to cure epoxy resin bonded magnets. The bonded magnets prepared from the $\text{Zn}/\text{Sm}_2\text{Fe}_{17}\text{N}_x$ powders provided the highest $(\text{BH})_{\text{max}}$ value ($\sim 176 \text{ kJ m}^{-3}$) among the values reported up to date, even after exposure to air, and their irreversible flux loss was also smaller than that of the uncoated one.

Introduction

Recently, a rare earth-transition metal intermetallic compound, $\text{Sm}_2\text{Fe}_{17}\text{N}_x$ ($x = \sim 3$), has attracted much attention as a candidate for new high-performance permanent magnets because of its excellent magnetic properties.^{1,2} The saturation magnetization ($M_s = 1.57 \text{ T}$) of $\text{Sm}_2\text{Fe}_{17}\text{N}_x$ is almost comparable to that of $\text{Nd}_2\text{Fe}_{14}\text{B}$ ($M_s = 1.60 \text{ T}$), and the ideal $(\text{BH})_{\text{max}}$ value is as high as 490 kJ m^{-3} . In addition, the Curie temperature ($T_c = 747 \text{ K}$) is over 150 K higher than that of $\text{Nd}_2\text{Fe}_{14}\text{B}$ ($T_c = 586 \text{ K}$), and the anisotropy field ($H_a = 21 \text{ MA m}^{-1}$) is extremely huge. On the other hand, $\text{Sm}_2\text{Fe}_{17}\text{N}_x$ is metastable and decomposes at the temperature above 900 K, so that practical applications of this compound are limited to bonded magnets, which are generally produced by bonding the magnetic powder with a binder, for instance, an epoxy resin or a metal with low melting point such as zinc or tin.^{3–5} The main products in market are $\text{Sm}_2\text{Co}_{17}$ and $\text{Nd}_2\text{Fe}_{14}\text{B}$ epoxy resin bonded magnets, but their $(\text{BH})_{\text{max}}$ values are $\sim 130 \text{ kJ m}^{-3}$ at the largest. On the contrary, the $\text{Sm}_2\text{Fe}_{17}\text{N}_x$ -based bonded magnets are expected to provide much larger $(\text{BH})_{\text{max}}$ values than them owing to the inherent excellent magnetic property of $\text{Sm}_2\text{Fe}_{17}\text{N}_x$.

However, there are some problems in producing the $\text{Sm}_2\text{Fe}_{17}\text{N}_x$ -based bonded magnets with the excellent magnetic properties at the local for practical use. The coercivity mechanism of $\text{Sm}_2\text{Fe}_{17}\text{N}_x$ is controlled by a nucleation process,⁶ so that the high coercivity enough for practical use originates only from the microcrystalline $\text{Sm}_2\text{Fe}_{17}\text{N}_x$ samples prepared by means of rf sputtering,⁷ rapid quenching,⁸ and mechanical alloying.⁹ Since the materials obtained by these methods are magnetically isotropic or contain some soft magnetic phases, e.g., $\alpha\text{-Fe}$ and $\text{Sm}_2\text{Fe}_{17}$; however, the remanence (B_r) values of them are quite low. Magnetically anisotropic fine powder with high B_r value have been succeeded in obtaining from the coarse $\text{Sm}_2\text{Fe}_{17}\text{N}_x$ powder by grinding.^{10,11} Therefore, the grinding process is very important to prepare the powders with high B_r and H_{cj} values because these values depend upon not only the particle size but also the surface and bulk conditions of finely ground powders. A ball milling performed in a suitable solvent produces fine powder materials with inclusion of the less internal strain induced during the grinding process than by the other dry grinding method. However, powder particles of samples tend to aggregate one another and adhere on the surface of balls even in organic solvents. In addition, the fundamental mag-

* To whom correspondence should be addressed.

[®] Abstract published in *Advance ACS Abstracts*, November 1, 1997.

(1) Coey, J. M. D.; Sun, H. *J. Magn. Magn. Mater.* **1990**, *87*, L251.

(2) Li, H.-S.; Coey, J. M. D. In *Handbook of Magnetic Materials*; Buschow, K. H. J., Ed.; North-Holland: Tokyo, 1991; Vol. 6, Chapter 1.

(3) Huang, M. Q.; Zhang, L. Y.; Ma, B. M.; Zheng, Y.; Elbicki, J. M.; Wallace, W. E.; Sankar, S. G. *J. Appl. Phys.* **1991**, *70*, 6027.

(4) Kuhrt, C.; O'Donnell, K.; Katter, M.; Wecker, J.; Schnitzke, K.; Schultz, L. *Appl. Phys. Lett.* **1992**, *60*, 3316.

(5) Suzuki, S.; Miura, T.; Kawasaki, M. *IEEE Trans. Magn.* **1993**, *29*, 2815.

(6) Schnitzke, K.; Schultz, L.; Wecker, J.; Katter, M. *Appl. Phys. Lett.* **1990**, *57*, 2853.

(7) Rani, R.; Hedge, H.; Navarathna, A.; Cadien, F. J. *J. Appl. Phys.* **1993**, *73*, 6023.

(8) Katter, M.; Wecker, J.; Schultz, L. *J. Appl. Phys.* **1991**, *70*, 3188.

(9) Kou, X.; Qiang, W.; Kronmüller, H.; Schultz, L. *J. Appl. Phys.* **1993**, *74*, 6791.

(10) Tajima, S.; Hattori, T.; Kato, Y. *IEEE Trans. Magn.* **1995**, *31*, 3701.

(11) Machida, K.; Shiomi, A.; Izumi, H.; Adachi, G. *Jpn. J. Appl. Phys.* **1995**, *34*, L741.

netic values (B_r , H_{cj} , and $(BH)_{max}$) of the resulting fine powders tend to deteriorate because they are easily oxidized by air or water for the high reactivity. Therefore, it is necessary that the $Sm_2Fe_{17}N_x$ fine powders are protected from oxidation by isolating from air-water.

Otani et al.¹² have reported that the H_{cj} values of zinc metal bonded $Sm_2Fe_{17}N_x$ magnets are markedly improved since soft magnetic phases such as α -Fe, which play a role as nucleation point, are removed by reacting with zinc metal to produce paramagnetic phases such as Zn_7Fe_3 . However, a considerable amount of zinc metal is needed to produce such zinc metal bonded magnets to improve the H_{cj} value, so that the B_r value is depressed by a decrease of effective amount of $Sm_2Fe_{17}N_x$ although the H_{cj} value was increased. Therefore, if the surface of $Sm_2Fe_{17}N_x$ fine powders can be uniformly covered with a small amount of zinc metal, high-performance bonded magnets with good oxidation resistance should be fabrication.

In this study, a new grinding procedure based on ball milling in organic solutions containing a surfactant is applied to prepare the fine powders of $Sm_2Fe_{17}N_x$, and the powders are stabilized by surface coating with the zinc metal produced via photodecomposition of diethylzinc ($Zn(C_2H_5)_2$). Furthermore, their magnetic characteristics are investigated from the viewpoint of the practical use as permanent magnets.

Experimental Section

Preparation. The starting $Sm_2Fe_{17}N_x$ coarse powder was prepared by heating Sm_2Fe_{17} powder in a NH_3 - H_2 mixed gas (molar ratio = 1:2) and annealing at 723 K for a few hours in Ar to homogenize the distribution of nitrogen atoms in the crystal lattice and optimize the nitrogen content to $x = 3$ according to a procedure described elsewhere.¹³ By the latter treatment, the extra nitrogen and hydrogen stored in the $Sm_2Fe_{17}N_x$ powder during the nitrogenation were removed, and the resulting $Sm_2Fe_{17}N_3$ materials provided the high magnetic property. The raw coarse powders (particle size = 50–100 μm) was ground by ball milling in an n -hexane solution containing Aerosol OT (bis(2-ethylhexyl)sodium sulfosuccinate ($C_{20}H_{37}O_4SO_3Na$, 800 mL) using a glass pot (100 mm i.d. \times 150 mm) and steel balls (12 mm i.d., 325 g). The n -hexane used here was distilled in the presence of Na metal to remove water residue and all the manipulations were carried out in a purified Ar or N_2 atmosphere. After the ball milling, the n -hexane solution was removed by decantation and the powder samples were washed several times with the distilled n -hexane.

Platy samples of the $Sm_2Fe_{17}N_x$ were obtained by plasma nitrogenation of Sm_2Fe_{17} plate method in a N_2 - H_2 mixed gas,¹⁴ since the above nitrogenation in the NH_3 - H_2 mixture resulted in pulverization of the Sm_2Fe_{17} plates. The plasma nitrogenation efficiently took place only in the surface region of particles ($\sim 30 \mu m$), but their surface nitrogen compositions estimated on the basis of Auger electron spectroscopy (AES) measurements was almost equal to $Sm_2Fe_{17}N_3$.

The zinc coating was performed by two different procedures, i.e., chemical solution deposition (CSD) and chemical vapor deposition (CVD) methods (see Figure 1). For the CSD method, the powder (6 g) or plate ($10 \times 5 \times 3$ mm) samples were put into a quartz cell (5 mm i.d. \times 70 mm) and added 20

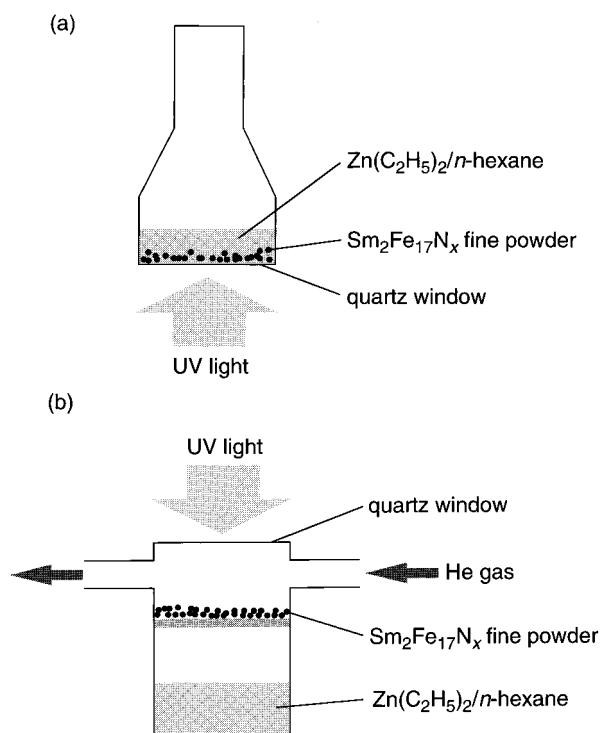


Figure 1. Glass cells for the zinc coating by (a) CSD and (b) CVD methods.

mL of an n -hexane solution containing 13.1 mol % $Zn(C_2H_5)_2$. For the CVD method, the $Sm_2Fe_{17}N_x$ powder (2 g) or plate samples were put on a glass filter (80 mm i.d.) of the cell (80 mm i.d. \times 100 mm) while the n -hexane solution containing $Zn(C_2H_5)_2$ (13.1 mol %) was introduced in a lower part of the cell. Decomposition of $Zn(C_2H_5)_2$ was performed by irradiation of UV light for 5–10 h using a low-pressure mercury arc at room temperature in an inert atmosphere (Ar or He). Particularly, the surface coating by the CSD method was performed on the $Sm_2Fe_{17}N_x$ fine particles by agitating them using an ultrasonic wave generator every 10 min in order to make uniform zinc films. The resulting $Zn/Sm_2Fe_{17}N_x$ samples were washed three times with the distilled n -hexane and dried.

Compression-type bonded magnets were made by mixing the resulting $Zn/Sm_2Fe_{17}N_x$ powder with 2.5 wt % of an epoxy resin, molding under pressure of 1.4 GPa in magnetic field of 1.4 MA m^{-1} , and heating for cure at 353 K for 4 h. The same bonded magnets prepared from the uncoated $Sm_2Fe_{17}N_x$ powder as reference. Density of the bonded magnets was measured by the Archimédés method, and their values were distributed between 5.8 and 6.0 $g\ cm^{-3}$.

Characterization. The $Sm_2Fe_{17}N_x$ samples were identified on the basis of X-ray diffraction (XRD) patterns measured using Cu $K\alpha$ radiation, and the nitrogen and oxygen contents were checked on a nitrogen and oxygen analyzer (Horiba, EMGA-550). Qualitative and quantitative analysis for the sodium and zinc derived from Aerosol OT and $Zn(C_2H_5)_2$ were performed with inductively coupled plasma atomic emission spectroscopy apparatus (Shimadzu, ICPS-1000IV). Relative surface area values of the samples were measured by the BET method at 77 K. The orientation behavior based on the magnetic anisotropy of $Sm_2Fe_{17}N_x$ fine powders was characterized by XRD measurements on aligned samples in a magnetic field of 1.4 MA m^{-1} . Auger electron spectra of the zinc-coated platy samples were obtained on an X-ray photoelectron spectroscopy apparatus (Physical Electronics, Model-5500MT). Magnetization hysteresis curves of the powder and bonded samples were recorded on a vibrating sample magnetometer (Toei, VSM-5-15) in a range of magnetic field up to ± 1.2 MA m^{-1} at room temperature after a magnetization at 4.8 MA m^{-1} by a pulsed field generator.

(12) Otani, Y.; Moukarika, A.; Sun, H.; Coey, J. M. D.; Devlin, E.; Harris, I. R. *J. Appl. Phys.* **1991**, *69*, 6735.

(13) Kobayashi, K.; Iriyama, T.; Imaoka, N.; Kashiwaya, N. European Patent Appl. No. 0-417-732-42, 1990.

(14) Machida, K.; Nakamoto, A.; Adachi, G. *Chem. Mater.* **1994**, *6*, 2103.

Table 1. Magnetic Property and Oxygen Content of $\text{Sm}_2\text{Fe}_{17}\text{N}_x$ Powder

surfactant ^a (wt %)	milling time (h)	oxygen content (wt %)	magnetic properties					specific surface area ($\text{m}^2 \text{g}^{-1}$)
			M_s (T)	B_r (T)	H_{cj} (MA m^{-1})	H_k/H_{cj}	$(\text{BH})_{\text{max}}$ (kJ m^{-3})	
0	72	0.81	1.18	1.00	0.63	0.30	156	1.60
5	18	0.59	1.39	1.37	0.86	0.56	313	0.24
5	72	0.99	1.32	1.28	1.13	0.33	258	0.66

^a Aerosol OT ($\text{C}_{20}\text{H}_{37}\text{O}_4\text{SO}_3\text{Na}$).

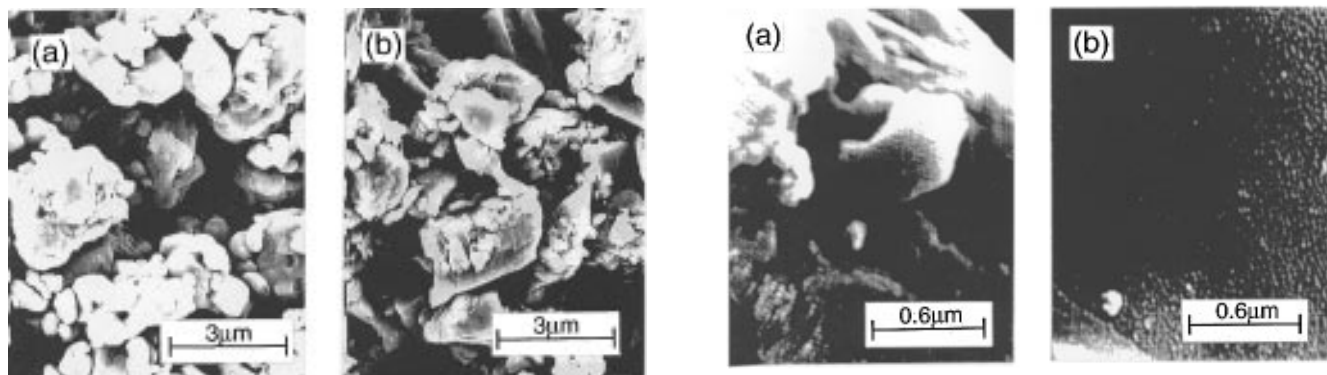


Figure 2. SEM micrographs of the $\text{Sm}_2\text{Fe}_{17}\text{N}_x$ powders prepared by ball milling in *n*-hexane solution (a) without Aerosol OT for 72 h and (b) with it for 18 h.

Results and Discussion

Fine Grinding. The $\text{Sm}_2\text{Fe}_{17}\text{N}_x$ powder tended to aggregate and to adhere to steel balls during milling in pure *n*-hexane (surfactant free), and it was difficult to collect the ground powder from the glass pot and steel balls. On the other hand, it was found that the ball milling in the *n*-hexane solution containing Aerosol OT was a good procedure to grind the $\text{Sm}_2\text{Fe}_{17}\text{N}_x$ coarse powder. Figure 2 shows typical SEM micrographs for the ground $\text{Sm}_2\text{Fe}_{17}\text{N}_x$ fine powders. Although the $\text{Sm}_2\text{Fe}_{17}\text{N}_x$ fine powders ground for 72 h in pure *n*-hexane (Figure 2a) and for 18 h in the *n*-hexane solution containing 5 wt % of Aerosol OT (Figure 2b) had almost a similar mean particle size (ca. 2 μm) to each other, the B_r and H_{cj} values and the oxygen content were quite different from one another (see Table 1). The B_r and H_{cj} values for the latter sample were 1.36 T and 1.08 MA m^{-1} , whereas the values of the former one were 1.00 T and 0.63 MA m^{-1} , respectively. Consequently, the $(\text{BH})_{\text{max}}$ value of the latter powder (313 kJ m^{-3}) was improved to twice as large as that of the former sample (156 kJ m^{-3}). A rectangularity refined as H_k/H_{cj} (where H_k is a coercivity value at $M = 0.9B_r$) were evaluated to be 0.30 and 0.56 for the $\text{Sm}_2\text{Fe}_{17}\text{N}_x$ fine powders ground in the surfactant-free and charged *n*-hexane, respectively. This indicates that the former $\text{Sm}_2\text{Fe}_{17}\text{N}_x$ fine particles tend to aggregate compared with the latter ones, owing to the wide particle size distribution of the former powder. Therefore, the fundamental magnetic characteristics, particularly the B_r and $(\text{BH})_{\text{max}}$ values, are considerably improved by depressing the aggregation among the $\text{Sm}_2\text{Fe}_{17}\text{N}_x$ fine particles prepared by ball milling in the organic solution containing Aerosol OT.

On the other hand, the specific surface area (0.24 $\text{m}^2 \text{g}^{-1}$) and oxygen content (0.59 wt %) of the $\text{Sm}_2\text{Fe}_{17}\text{N}_x$ fine powder ground for 18 h in the *n*-hexane solution containing 5 wt % of Aerosol OT were maintained better at the lower level than those of the former sample

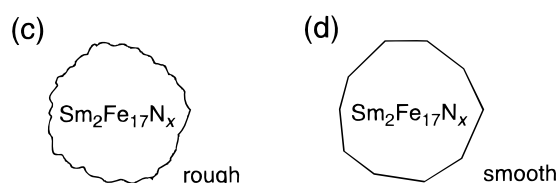


Figure 3. Highly magnified SEM micrographs of the $\text{Sm}_2\text{Fe}_{17}\text{N}_x$ fine powders a and b denoted in Figure 2, and schematic illustrations of the corresponding typical particles c and d.

ground for 72 h under the surfactant-free condition (1.60 $\text{m}^2 \text{g}^{-1}$ and 0.81 wt %). Highly magnified SEM micrographs for two kinds of the $\text{Sm}_2\text{Fe}_{17}\text{N}_x$ fine powders are shown in Figure 3. One can see from the photographs that their surface morphologies are considerably different from each other: The $\text{Sm}_2\text{Fe}_{17}\text{N}_x$ particles ground without the surfactant provided a much rougher surface compared with the powders prepared using the surfactant because the $\text{Sm}_2\text{Fe}_{17}\text{N}_x$ particles were rubbing one another or adhered to the surface of steel balls during the milling in pure *n*-hexane. For the $\text{Sm}_2\text{Fe}_{17}\text{N}_x$ fine powders ground using the surfactant, the surface was much smoother than that of the samples ground without the surfactant. This is supported by their surface area values which significantly differ from each other: 1.60 $\text{m}^2 \text{g}^{-1}$ for the surfactant-free sample and 0.24 $\text{m}^2 \text{g}^{-1}$ for the surfactant-charged sample, although their mean particle sizes are equal to each other (ca. 2 μm). The surfactant seems to have an effect on prevention from the aggregation among the $\text{Sm}_2\text{Fe}_{17}\text{N}_x$ particles during the ball milling using the formation of reversed micelles around them and reduction of the mechanical strength for the powder particles (Rehbinder effect¹⁵). Therefore, the $\text{Sm}_2\text{Fe}_{17}\text{N}_x$ fine powders with the much smoother surface provide the better oxidation resistivity than the samples ground without the surfactant, and consequently they show the more excellent magnetic property.

Surfactant concentration dependences of the B_r , H_{cj} , and $(\text{BH})_{\text{max}}$ values for the $\text{Sm}_2\text{Fe}_{17}\text{N}_x$ fine powder

(15) Rehbinder, P. A. *Z. Phys.* **1931**, 72, 191.

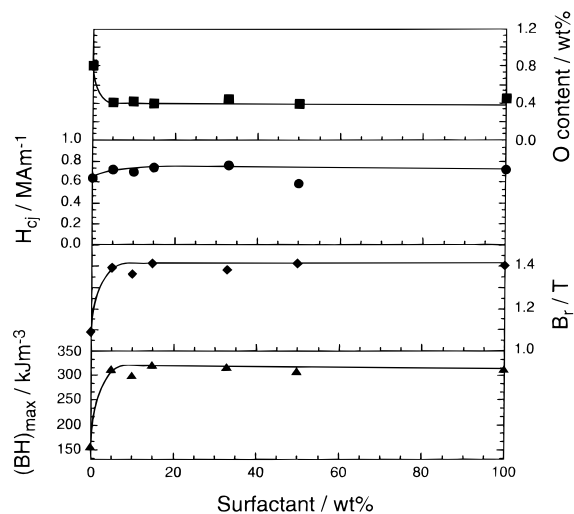


Figure 4. Surfactant concentration dependence of the oxygen content and magnetic property for the $\text{Sm}_2\text{Fe}_{17}\text{N}_x$ fine powder ground by ball milling. Milling time: 12 h.

ground for 12 h in the *n*-hexane solutions containing various amounts of Aerosol OT are shown in Figure 4, together with that of the oxygen content. The results at a surfactant concentration of zero were obtained from the sample ground for 72 h in pure *n*-hexane (surfactant-free). By addition of the surfactant, the ball milling for the $\text{Sm}_2\text{Fe}_{17}\text{N}_x$ coarse powder more smoothly took place than the case of surfactant-free grinding and the fundamental magnetic property of the resulting fine powders was considerably improved compared with those of the surfactant-free samples. In addition, it was found from the flatness of these surfactant concentration dependences that even the small amount of surfactant (only 5 wt %) was enough to form the reversed micelles of Aerosol OT around the $\text{Sm}_2\text{Fe}_{17}\text{N}_x$ fine particles with a mean particle size of ca. 3 μm . Therefore, it is concluded that the oxygen content and magnetic property of the $\text{Sm}_2\text{Fe}_{17}\text{N}_x$ fine powders ground using Aerosol OT are independent of its concentration in the *n*-hexane solution as well as their particle sizes.

Figure 5 shows milling time dependences of the B_r , H_{cj} , and $(\text{BH})_{\text{max}}$ values of the $\text{Sm}_2\text{Fe}_{17}\text{N}_x$ fine powders ground in the *n*-hexane solution containing 5 wt % of Aerosol OT, together with that of the oxygen content. The oxygen content and H_{cj} value increased with the milling time while the B_r value was inversely decreased. Therefore, the resulting $(\text{BH})_{\text{max}}$ value was maximized at a milling time around 12 h. The mean particle size for the fine powder milled for 12 h was evaluated to be around 3 μm from the SEM observation and 3.5 μm by the calculation based on the specific surface area (0.23 $\text{m}^2 \text{g}^{-1}$). A single domain size of isolated spherical particle, R_c , is given as a critical radius by eq 1:¹⁶

$$R_c = 9\nu\mu_0/M_s^2 \quad (1)$$

where γ is the domain wall energy, μ_0 the permeability of vacuum, and M_s the saturation magnetization. The value γ is represented as $\gamma = 4(AK)^{1/2}$, where A is the average exchange constant and K the uniaxial anisotropy constant. The critical radius of single domain particle R_c was estimated to be 0.34 μm for the $\text{Sm}_2\text{Fe}_{17}\text{N}_x$

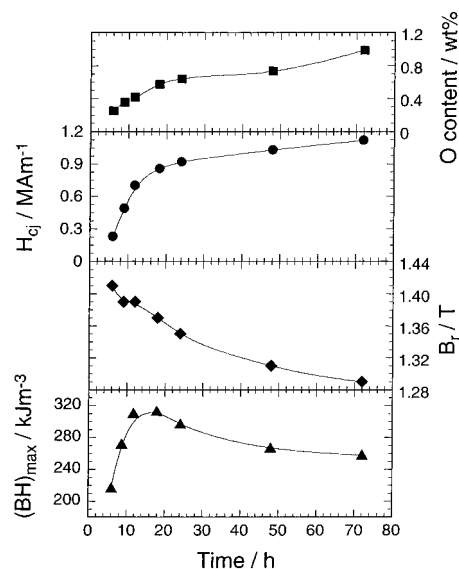


Figure 5. Milling time dependence of the oxygen content and magnetic property for the $\text{Sm}_2\text{Fe}_{17}\text{N}_x$ fine powder ground using Aerosol OT. Surfactant concentration: 5 wt %.

Fe_{17}N_x powder from eq 1 by substituting the following values: $M_s = 1.57 \text{ T}$ (theoretical one) and $\gamma = 7.4 \times 10^{-2} \text{ J m}^{-2}$.¹² The R_c value of a magnetic single domain for the polycrystalline $\text{Sm}_2\text{Fe}_{17}\text{N}_x$ particles is 2 times larger than that of isolated particles because the magnetostatic energy of the polycrystalline materials is smaller than that of the isolated particle,¹⁷ so that the radius of the single domain particle was estimated to be about 0.7 μm . It has been reported that the single domain size of $\text{Sm}_2\text{Fe}_{17}\text{N}_x$ is evaluated to be 1–2 μm from Kerr effect microscopy observation^{18,19} or 3–4 μm from transmission electron microscopy.²⁰ Therefore, the $\text{Sm}_2\text{Fe}_{17}\text{N}_x$ particles prepared here are almost ground up to the single domain size, and the higher coercivity can be achieved by further grinding. However, the B_r value decreased with milling time. This means that the specific surface area expands with decrease of the particle size, but the samples become easy to be oxidize owing to the increased surface energy of the particles. It has been reported that amorphous-like layers are formed on the surface of jet-milled $\text{Sm}_2\text{Fe}_{17}\text{N}_x$ fine powders, in which most of the oxygen is concentrated.²⁰ Since the oxygen content of the $\text{Sm}_2\text{Fe}_{17}\text{N}_x$ fine powders was increased certainly with the milling time, the same amorphous-like layers containing oxygen might also be produced on their surface. Therefore, the B_r value of the $\text{Sm}_2\text{Fe}_{17}\text{N}_x$ fine powders should be reduced because of the formation of amorphous-like layers. However, since such amorphous-like layers may not contribute to the magnetic property as the nucleation points,²⁰ the dependences of B_r and H_{cj} values on the milling time are contrary to each other as seen from Figure 5. Therefore, it is necessary to produce the $\text{Sm}_2\text{Fe}_{17}\text{N}_x$ fine powders which provide the well-balanced B_r and H_{cj} values resulting in high $(\text{BH})_{\text{max}}$ values. The high $(\text{BH})_{\text{max}}$ value of 313 kJ m^{-3} was obtained under the milling time condition of 12–18 h. Optimization of the

(17) Chikazumi, S. *Physics of Magnetism*; Wiley: New York, 1964.

(18) Mukai, T.; Fujimoto, T. *J. Magn. Magn. Mater.* **1990**, *103*, 165.

(19) Hu, J.; Dragon, T.; Sartorelli, M. L.; Kronmüller, H. *Phys. Status Solidi A* **1993**, *136*, 207.

(20) Kobayashi, K.; Iriyama, T.; Yamaguchi, T.; Kato, H.; Nakagawa, Y. *J. Alloys Compd.* **1993**, *193*, 235.

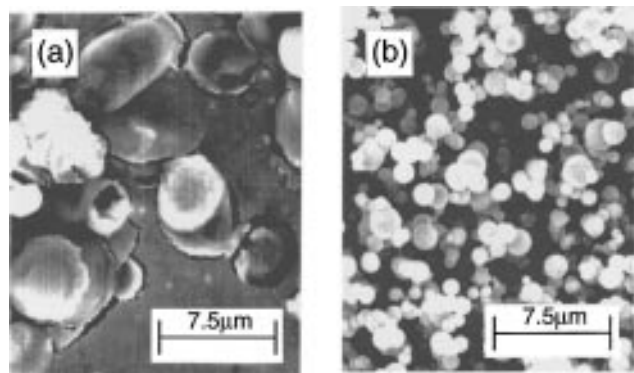
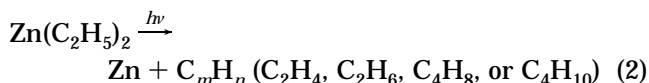


Figure 6. SEM micrographs of the platy samples coated with zinc metal by the (a) CSD and (b) CVD methods.

conditions, milling time, and amounts of surfactant, solvent, and steel balls resulted in the highest $(\text{BH})_{\text{max}}$ value around 330 kJ m^{-3} .

Tajima et al. have made the comment that alkali or alkaline-earth metal ion-free surfactants should be used for the ball milling of $\text{Sm}_2\text{Fe}_{17}\text{N}_x$ powders because such metal ions influence the magnetic property as contaminants.²¹ However, any sodium ion derived from the surfactant (Aerosol OT) used here was not detected on the resulting $\text{Sm}_2\text{Fe}_{17}\text{N}_x$ fine powders even by the ICP measurements. Therefore, one can also use conventional surfactants containing alkali or alkaline-earth metal ions such as Aerosol OT for the ball milling of $\text{Sm}_2\text{Fe}_{17}\text{N}_x$ material.

Zinc Metal Coating. Diethylzinc ($\text{Zn}(\text{C}_2\text{H}_5)_2$) absorbs UV lights around 214.5 nm and decomposes according to eq 2:



This reaction scheme suggests that the surface of the $\text{Sm}_2\text{Fe}_{17}\text{N}_x$ fine particles is coated with the resulting Zn metal and the hydrocarbons (C_mH_n) evolved as byproducts are also too inert to react with $\text{Sm}_2\text{Fe}_{17}\text{N}_x$. SEM micrographs observed on the $\text{Sm}_2\text{Fe}_{17}\text{N}_x$ plates coated with the zinc metal produced via the photodecomposition of $\text{Zn}(\text{C}_2\text{H}_5)_2$ by the CSD and CVD methods ($\text{Zn}/\text{Sm}_2\text{Fe}_{17}\text{N}_x$) are shown in Figure 6. The CSD sample was covered by the zinc film with a cracked rough surface, while the surface of the CVD sample was uniformly covered with a number of small zinc particles. Significant amounts of zinc ($\sim 1 \text{ wt } \%$) were detected from the $\text{Zn}/\text{Sm}_2\text{Fe}_{17}\text{N}_x$ fine powders coated by the CSD method by fluorescent X-ray analysis measurements on a micron scale. Electron probe microanalysis maps showed that zinc was uniformly distributed as a thin film on the $\text{Sm}_2\text{Fe}_{17}\text{N}_x$ fine powders. For the CVD samples, however, the amounts of the zinc coated on the surface of the $\text{Sm}_2\text{Fe}_{17}\text{N}_x$ fine particles ($\sim 0.6 \text{ wt } \%$) were somewhat smaller than those of the CSD samples. This is due to that the UV light intensity was gradually weakened with irradiation time because the zinc film was also formed on an inner side surface of the quartz window attached at the top of the glass cell (see Figure 1) and the UV light became hard to permeate through

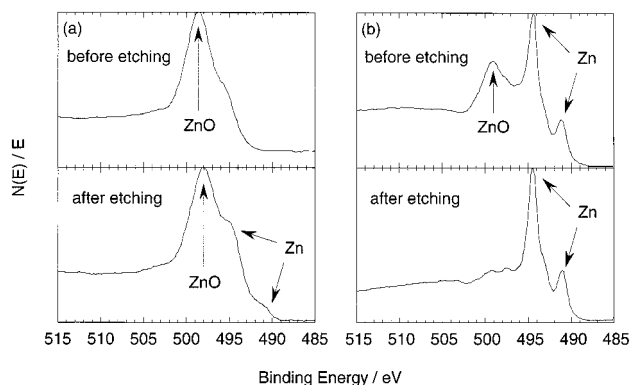


Figure 7. AES profiles of the platy samples a and b denoted in Figure 6.

it, although the UV irradiation for both the CSD and CVD methods lasted for the same time (5 h).

Diethylzinc can also release the zinc metal by a thermal or plasma-induced decomposition method. However, since the hydrocarbons evolved as byproducts via the decomposition of $\text{Zn}(\text{C}_2\text{H}_5)_2$ were also decomposed by themselves at the same time under the conditions of these methods, the resulting carbon fractions contaminated the $\text{Zn}/\text{Sm}_2\text{Fe}_{17}\text{N}_x$ materials. Therefore, these methods are not available to prepare the zinc films from $\text{Zn}(\text{C}_2\text{H}_5)_2$ compared with the photoinduced decomposition method denoted as the CSD or CVD ones.

Figure 7 shows AES profiles of the CSD and CVD samples before and after etching for 5 nm (converted to SiO_2). The AES profile of the unetched CSD sample was completely assigned to the Zn LMM signal derived from ZnO (499.0 eV). After the etching, however, two shoulder peaks appeared at 491.0 and 494.5 eV, which were assigned to the Zn LMM signals of zinc metal. On the other hand, AES profiles of the as-prepared CVD samples consisted of several peaks originating from zinc metal and ZnO even before such surface etching. However, after the etching, the peaks assigned to zinc metal were considerably intensified and sharpened while the peak of ZnO almost disappeared. In addition, the respective peak intensity ratios of the O 1s signal vs the Zn 2p one for the CSD sample before and after the etching were 0.72 and 0.67, while the ratio for the CVD sample considerably decreased from 0.69 to 0.24 through the etching. Diethylzinc releases the zinc metal on the surface of the $\text{Sm}_2\text{Fe}_{17}\text{N}_x$ particles in the case of CSD procedure (see Figure 8a). On the other hand, for the CVD procedure, nuclei of zinc metal derived from the decomposition of $\text{Zn}(\text{C}_2\text{H}_5)_2$ were grown, and the resulting fine particles of zinc metal covered minutely the surface of the $\text{Sm}_2\text{Fe}_{17}\text{N}_x$ fine particles (see Figure 8b). The zinc films coated by both the CSD and CVD methods were partly oxidized during the sample manipulation. Furthermore, the zinc film obtained by the CVD procedure is expected to provide a better oxidation resistivity than the CSD one.

On the other hand, the CVD method employed in this work was a static process and was not able to perform the uniform coating on the surface of the $\text{Sm}_2\text{Fe}_{17}\text{N}_x$ fine particles because their shadow (lower) side was hardly coated with zinc metal (see Figure 1). Therefore, the CVD method at this stage cannot provide the $\text{Zn}/\text{Sm}_2\text{Fe}_{17}\text{N}_x$ powder with enough stability to use practically.

X-ray diffraction (XRD) patterns of the $\text{Zn}/\text{Sm}_2\text{Fe}_{17}\text{N}_x$ fine powder with a mean diameter below $3 \mu\text{m}$ were

(21) Tajima, S.; Hattori, T.; Kato, Y. *J. Magn. Soc. Jpn.* **1995**, *19*, 221.

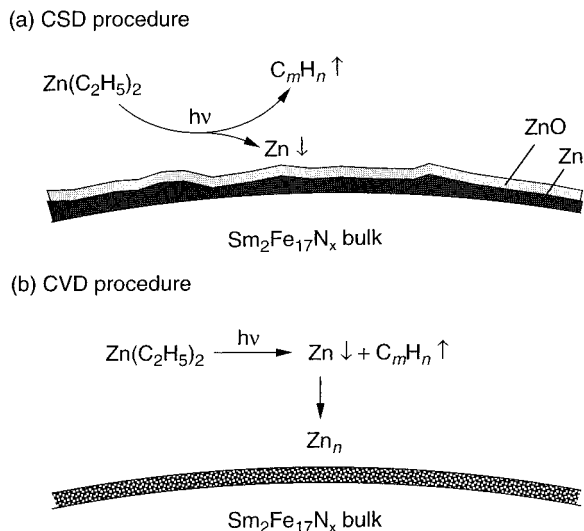


Figure 8. Proposed models of the zinc films coated on the surface of $\text{Sm}_2\text{Fe}_{17}\text{N}_x$ particles by (a) CSD and (b) CVD methods.

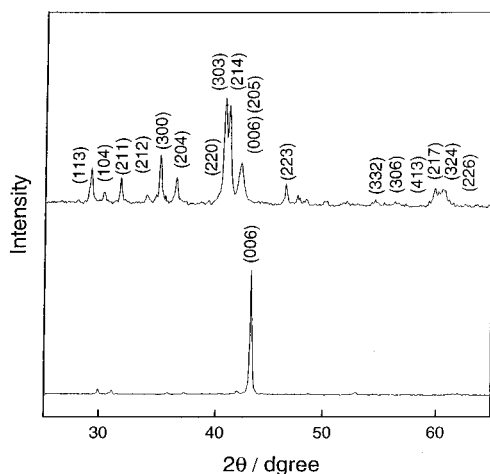


Figure 9. X-ray diffraction patterns ($\text{CuK}\alpha$ radiation) of the $\text{Zn}/\text{Sm}_2\text{Fe}_{17}\text{N}_x$ fine powder (a) before and (b) after magnetic alignment along a direction perpendicular to the sample plate in a magnetic field of ca. 14 kA m^{-1} .

obtained before and after alignment in a magnetic field along a direction perpendicular to the sample plate (see Figure 9). The XRD pattern measured before the magnetic alignment was fairly assigned on the basis of the crystal data reported on $\text{Sm}_2\text{Fe}_{17}\text{N}_x$ (space group $R\bar{3}m$, $a = 8.73$, $c = 12.64 \text{ \AA}$).² Particularly, since no extra peaks derived from α -Fe was observed, it was judged that the $\text{Zn}/\text{Sm}_2\text{Fe}_{17}\text{N}_x$ fine powder prepared here was free from the α -Fe phase. On the other hand, only a sharp (006) peak was observed after the magnetic alignment. This indicates that the $\text{Zn}/\text{Sm}_2\text{Fe}_{17}\text{N}_x$ fine powder shows a good magnetic anisotropy and behave as magnetic single domain particles.

Typical anisotropic magnetization hysteresis loops of the $\text{Zn}/\text{Sm}_2\text{Fe}_{17}\text{N}_x$ powder recorded along easy and hard directions are shown in Figure 10, together with an isotropic magnetization hysteresis with a virgin curve. It can be glanced from the virgin curve with no magnetic field for induction that the demagnetization process of $\text{Zn}/\text{Sm}_2\text{Fe}_{17}\text{N}_x$ powder takes place according to the nucleation mechanism, and the fact that the magnetization is easily saturated supports that the $\text{Zn}/\text{Sm}_2\text{Fe}_{17}\text{N}_x$ fine powder is of a single magnetic domain. After

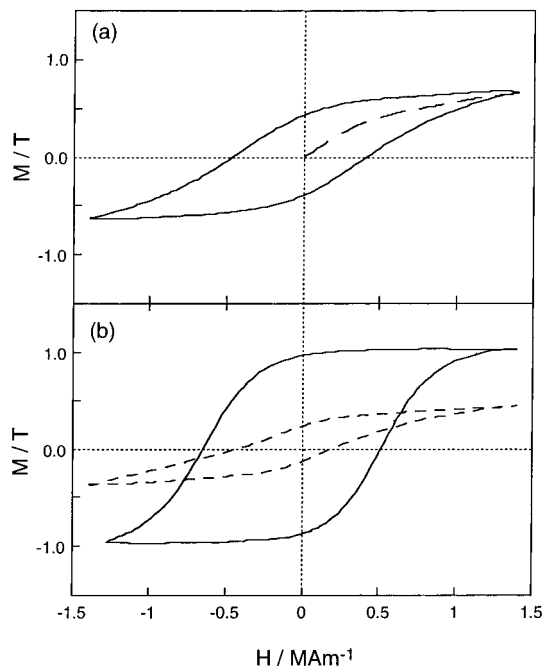


Figure 10. (A) Typical isotropic magnetization hysteresis loop of the $\text{Zn}/\text{Sm}_2\text{Fe}_{17}\text{N}_x$ fine powder with an initial magnetization curve of virgin sample and (B) anisotropic loops recorded along easy (solid line) and hard (dash line) directions of the aligned powder.

alignment of the $\text{Zn}/\text{Sm}_2\text{Fe}_{17}\text{N}_x$ powder, the magnetic anisotropy were clearly observed between the magnetization loops measured along the easy and hard directions. The resulting remanence factor ratio $(B_r)_{\text{easy}}/(B_r)_{\text{hard}}$ was 4.9.

A series oxygen content and fundamental magnetic data observed on the $\text{Sm}_2\text{Fe}_{17}\text{N}_x$ fine powders with and without the zinc coating are listed in Table 2, together with those of the samples heated at various temperatures in Ar. Heating time dependences of oxygen content and fundamental magnetic property for the uncoated $\text{Sm}_2\text{Fe}_{17}\text{N}_x$ and coated $\text{Zn}/\text{Sm}_2\text{Fe}_{17}\text{N}_x$ fine powders are shown in Figure 11. For the uncoated $\text{Sm}_2\text{Fe}_{17}\text{N}_x$ sample, since the oxygen content was markedly increased, the B_r and H_{cj} values were inversely decreased by heat treatment at 423 K. On the other hand, both the $\text{Zn}/\text{Sm}_2\text{Fe}_{17}\text{N}_x$ powders coated with the CSD and CVD methods provided only small rates of increase for the oxygen content even after the heat treatment at the same temperature, which was enough to cure the epoxy resin bonded magnets ($T > 350 \text{ K}$), and the fundamental magnetic parameters were retained at high levels, respectively. Although it has been reported that zinc metal improves the H_{cj} value of $\text{Sm}_2\text{Fe}_{17}\text{N}_x$ material owing to neutralizing the nucleation points (mainly α -Fe) by formation of paramagnetic Zn-Fe intermetallic compounds such as Zn_7Fe_3 via the reaction between Zn metal and α -Fe,³⁻⁵ the H_{cj} values of the $\text{Zn}/\text{Sm}_2\text{Fe}_{17}\text{N}_x$ fine powders unheated and heated at the temperature less than 423 K are almost at the same level as each other. This result means that the zinc metal coating film covers only the surface of $\text{Sm}_2\text{Fe}_{17}\text{N}_x$ fine particle to protect from the oxidation and does not react with α -Fe to produce the Zn-Fe compound that can enhance the H_{cj} value.

On the other hand, it is expected that such a Zn-Fe compound is formed at temperatures above 423 K.

Table 2. Magnetic Property and Oxygen Content of $\text{Sm}_2\text{Fe}_{17}\text{N}_x$ and $\text{Zn}/\text{Sm}_2\text{Fe}_{17}\text{N}_x$ Powders^a without and with Zinc Coating

zinc coating	heat treatment		oxygen content (wt %)	coercivity (MA m^{-1})	remanence (T)	maximum energy product (kJ m^{-3})
	temp (K)	time (h)				
none	none	none	0.59	0.86	1.37	313
none	423	1	0.88	0.84	1.12	182
none	423	10	1.06	0.40	0.75	69
CSD	none	none	0.56	0.84	1.35	300
CSD	423	1	0.54	0.82	1.35	295
CSD	423	10	0.55	0.76	1.38	309
CSD	523	1	0.57	0.62	1.26	236
CSD	623	1	0.53	0.57	0.83	95
CSD	723	1	0.55	0.60	0.78	88
CVD	none	none	0.43	0.68	1.31	286
CVD	423	1	0.58	0.69	1.30	272
CVD	423	10	0.57	0.68	1.25	258
CVD	523	1	0.38	0.62	1.33	292
CVD	623	1	0.46	0.42	1.13	192
CVD	723	1	0.52	0.42	0.80	102

^a The ball milling was made for 18 h and the mean particle size was ca. 2 μm .

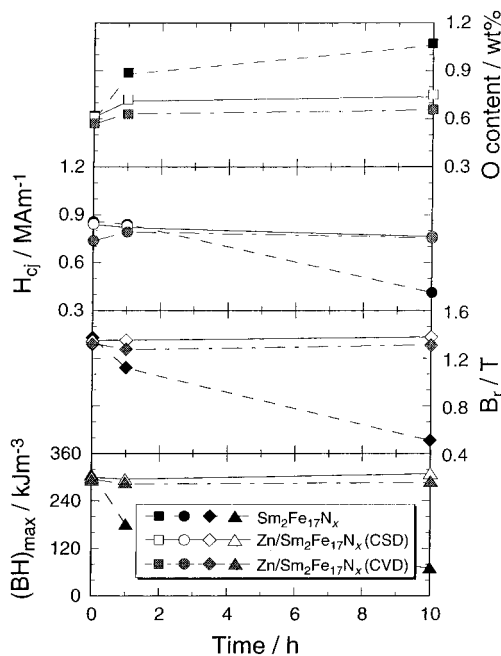
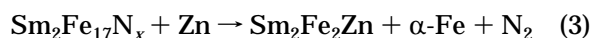


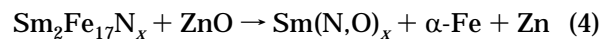
Figure 11. Heating time dependence of the oxygen content and magnetic property of the uncoated $\text{Sm}_2\text{Fe}_{17}\text{N}_x$ and coated $\text{Zn}/\text{Sm}_2\text{Fe}_{17}\text{N}_x$ fine powders with zinc metal by the CSD and CVD methods. Heating treatment: in Ar, 423 K.

However, when the temperature for heat treatments was elevated above 423 K, the B_r and H_{cj} values for the coated $\text{Zn}/\text{Sm}_2\text{Fe}_{17}\text{N}_x$ fine powders were inversely lowered, although their oxygen contents were scarcely changed (see Table 2). For zinc metal-bonded magnets, large amounts of the zinc metal are necessary for binding together $\text{Sm}_2\text{Fe}_{17}\text{N}_x$ fine powders and can improve the H_{cj} value because the zinc metal added fully reacts with $\alpha\text{-Fe}$, although the additional iron metal ($\alpha\text{-Fe}$) also produced via the reaction between $\text{Sm}_2\text{Fe}_{17}\text{N}_x$ and Zn at the temperature around the melting point of zinc according to eq 3:²²



However, since the zinc film as especially obtained by the CSD method consists of mixtures of zinc metal and

ZnO , $\text{Sm}_2\text{Fe}_{17}\text{N}_x$ is expected to be oxidized by reacting with ZnO : The oxygen in the zinc film migrates to the $\text{Sm}_2\text{Fe}_{17}\text{N}_x$ particle bulk and partly decomposes $\text{Sm}_2\text{Fe}_{17}\text{N}_x$ at temperatures below the melting point of zinc as shown in eq 4:



Therefore, although the H_{cj} value of the coated $\text{Zn}/\text{Sm}_2\text{Fe}_{17}\text{N}_x$ fine powders might be expected to be recovered by the heat treatments at 523–723 K because of the formation of paramagnetic Zn–Fe intermetallic compounds, we have never observed such enhancement on H_{cj} . On the other hand, the H_{cj} value was gradually decreased even for the coated $\text{Zn}/\text{Sm}_2\text{Fe}_{17}\text{N}_x$ fine powders. This may be due to the crystallization of the amorphous-like layers, $a\text{-Sm}_2\text{Fe}_{17}(\text{N},\text{O})_x$, formed on the surface of the $\text{Sm}_2\text{Fe}_{17}\text{N}_x$ fine powders as discussed later.

One is anxious about the CVD method that the surface of the $\text{Sm}_2\text{Fe}_{17}\text{N}_x$ fine particles cannot be uniformly covered by the zinc metal film prepared by this method because the decomposition of $\text{Zn}(\text{C}_2\text{H}_5)_2$ vapor does not take place on the shadow area of the particles (bottom side), and thus the further oxidation might still occur at such an uncoated area. This can be seen from the gradual increase of oxygen content for the CVD samples with increase of the heating time and temperature (see Table 2). Therefore, if the whole surface of the $\text{Sm}_2\text{Fe}_{17}\text{N}_x$ particles can be completely coated with the zinc metal produced by the CVD method, the oxidation resistance of the $\text{Sm}_2\text{Fe}_{17}\text{N}_x$ fine powders should be improved much more.

Magnetic Properties of Bonded Magnets. Demagnetization curves for the $\text{Zn}/\text{Sm}_2\text{Fe}_{17}\text{N}_x$ powder prepared by the CSD method and its bonded magnet were shown in Figure 12. It can be judged from the B_r value of the bonded magnet that the $\text{Zn}/\text{Sm}_2\text{Fe}_{17}\text{N}_x$ powder has not been seriously damaged during pressing and curing to produce the bonded magnets because the B_r value is consistent with the calculate one by taking into account the reduced density value by dilution with the epoxy resin used in this work. However, the H_{cj} value was decreased during the pressing, curing, and subsequent standing in air. The reduction of H_{cj} caused by the pressing should be due the crystal lattice of

(22) Wendhausen, P. A. P.; Hu, B.; Handstein, A.; Eckert, D.; Pitschke, W.; Müller, K.-H. *IEEE Trans. Magn.* **1993**, *29*, 2824.

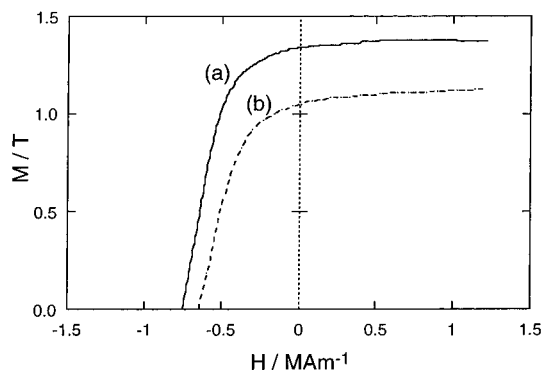
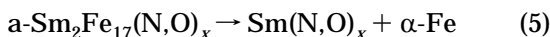


Figure 12. Demagnetization curves for (a) starting Zn/Sm₂Fe₁₇N_x powder and (b) its bonded magnets. The zinc coating was made by the CSD method.

grains being distorted to induce an internal stress by the applied uniaxial pressing of 1.4 GPa. The further decrease of the H_{cj} value even after the molding is responsible for the crystallization of the amorphous-like layers rich in oxygen, α -Sm₂Fe₁₇(N,O)_x, to produce the soft phase of α -Fe on the surface of Sm₂Fe₁₇N_x fine particles as follows:



The rectangularity of bonded magnets was also lowered compared with that of the starting Zn/Sm₂Fe₁₇N_x fine powder because the orientation of the particles was disordered during pressing. Nevertheless, the bonded magnets made from the CSD powder provided $(\text{BH})_{\text{max}} = 176 \text{ kJ m}^{-3}$, which was the highest value among those as reported to date, e.g., 164 kJ m^{-3} ,²³ even after exposure to air.

Exposure time dependences of the magnetic property for the uncoated Sm₂Fe₁₇N_x and coated Zn/Sm₂Fe₁₇N_x bonded magnets are shown in Figure 13. The magnetic property for the uncoated Sm₂Fe₁₇N_x bonded magnet after standing in air at room temperature for 15 days was considerably poor compared with the initial one. On the contrary, the B_r and $(\text{BH})_{\text{max}}$ values for the coated Zn/Sm₂Fe₁₇N_x bonded magnets were retained at levels as high as the initial data for 15 days, and furthermore the reduction rate of these values for the CSD sample was also small even after 150 days, although the H_{cj} value was gradually decreased with standing time as well as those of other bonded magnets made from uncoated Sm₂Fe₁₇N_x or CVD-coated Zn/Sm₂Fe₁₇N_x fine powders. It is concluded that the coated Zn/Sm₂Fe₁₇N_x bonded magnets prepared from the CSD fine powders show good resistivity against further oxidation of the Sm₂Fe₁₇N_x particle bulk, which contributes to retaining the excellent magnetic property. However, the reduction of the H_{cj} value cannot be avoided by the surface coating with zinc metal because the amorphous-like layers, α -Sm₂Fe₁₇(N,O)_x, formed on the surface of Sm₂Fe₁₇N_x fine particles before the zinc metal coating may gradually crystallize to produce the magnetic soft phase, α -Fe, even at room temperature. Therefore, if the surface coating can be made before the formation of such amorphous-like layers, one should be expected to produce the Sm₂Fe₁₇N_x bonded magnets with a much more excellent magnetic property.

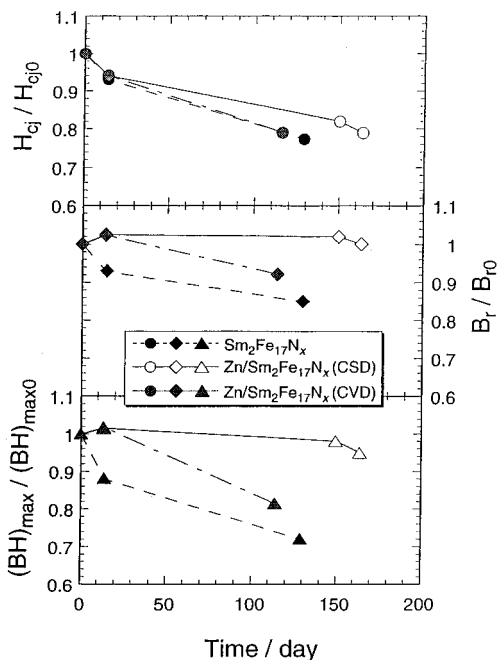


Figure 13. Exposure time dependences of the magnetic property for the uncoated Sm₂Fe₁₇N_x and coated Zn/Sm₂Fe₁₇N_x bonded magnets. Exposure condition: in air, at room temperature.

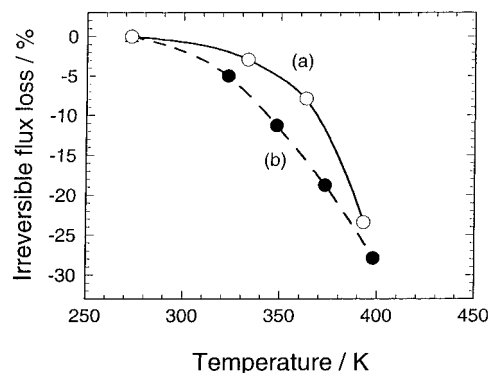


Figure 14. Irreversible flux loss curves for bonded magnets: (a) Zn/Sm₂Fe₁₇N_x (this work); (b) Sm₂Fe₁₇N_x (ref 24).

Figure 14 shows irreversible flux loss curves of the coated Zn/Sm₂Fe₁₇N_x (CSD) bonded magnet, together with that of uncoated Sm₂Fe₁₇N_x.²⁴ Iriyama et al. have reported that the irreversible flux loss of an uncoated Sm₂Fe₁₇N_x magnet after a heat treatment at 323 K in air is 5%,²⁴ and this is due to the serious oxidation of the Sm₂Fe₁₇N_x fine particles. For the coated Zn/Sm₂Fe₁₇N_x bonded magnet, however, the lower irreversible flux loss than 5% was still maintained even after heat treatment at the temperature around 348 K. This is attributed to the good oxidation resistance of the coated Zn/Sm₂Fe₁₇N_x fine powders, which allows them to be used as the bonded magnets at a higher temperature than the uncoated Sm₂Fe₁₇N_x fine powder.

Conclusions

The ball milling in the organic solution containing a suitable surfactant (e.g., Aerosol OT) is an efficient procedure to prepare the Sm₂Fe₁₇N_x fine powders with

(23) Imaoka, N.; Iriyama, T. *Denkigakkai-Kenkyukai-Shiryō* **1995**, *Mag-95-54*, 27.

(24) Iriyama, T.; Katsumata, T.; Mitsui, R. *Trans. Mater. Res. Soc. Jpn.* **1994**, *14B*, 1063.

excellent fundamental magnetic property. By addition of the surfactant, the aggregation among the raw $\text{Sm}_2\text{Fe}_{17}\text{N}_x$ coarse particles is effectively depressed by the formation of reversed micelles around them during the ball milling, so that the resulting $\text{Sm}_2\text{Fe}_{17}\text{N}_x$ fine powders are in a narrow particle size distribution and their surface is smooth compared with the powders ground under the surfactant-free condition. These characteristics resulted in lowering the number of nucleation points on the surface and improving the degree of orientation for the $\text{Sm}_2\text{Fe}_{17}\text{N}_x$ fine powders and consequently the excellent magnetic property, e.g., $(\text{BH})_{\text{max}} = \sim 330 \text{ kJ m}^{-3}$, occurs on them.

The surface coating for the $\text{Sm}_2\text{Fe}_{17}\text{N}_x$ fine powders with the zinc metal produced via the photodecomposition of $\text{Zn}(\text{C}_2\text{H}_5)_2$ in the solution phase (CSD method) improves the oxidation resistivity which is enough to produce the epoxy resin bonded magnets. The coated $\text{Zn}/\text{Sm}_2\text{Fe}_{17}\text{N}_x$ fine powders provides the magnetic parameters as high as the uncoated fresh samples even after the heat treatment at the temperature desired in the curing process for the bonded magnets (353–423 K) and also show the good rectangularity of $H_k/H_{\text{cj}} = 0.50\text{--}0.60$. The resulting bonded magnets give the most excellent permanent magnetic parameters among the uncoated $\text{Sm}_2\text{Fe}_{17}\text{N}_x$ magnets reported up to date, e.g., $(\text{BH})_{\text{max}}$ value = $\sim 176 \text{ kJ m}^{-3}$, which are maintained even in air for 150 days. However, the H_{cj} value was gradually decreased even for the coated $\text{Zn}/\text{Sm}_2\text{Fe}_{17}\text{N}_x$ bonded magnets. This may be due to the crystallization of the amorphous-like layers rich in oxygen, $\alpha\text{-Sm}_2\text{Fe}_{17}(\text{N},\text{O})_x$, formed on the surface of the $\text{Sm}_2\text{Fe}_{17}\text{N}_x$ fine

particles before the surface coating with zinc metal is made. This is supported by the results that the H_{cj} values is rapidly decreased by the heat treatment at the temperature above 423 K, e.g., 523 K, at which the crystallization of the amorphous layers should be enhanced, although at the same time, the migration of the oxygen in the amorphous-like layers and subsequent reaction with the $\text{Sm}_2\text{Fe}_{17}\text{N}_x$ particle bulk are also expected to be enhanced at that temperature. Therefore, if the surface of $\text{Sm}_2\text{Fe}_{17}\text{N}_x$ fine particles can be stabilized by the surface coating film of zinc metal before no amorphous-like layer rich in oxygen has been formed, then better bonded magnets than those fabricated in this work should be manufactured.

Acknowledgment. The authors wish to thank to Drs. T. Iriyama and N. Imaoka for their helpful suggestions regarding the preparation of raw powders and bonded magnets and Drs. K. Kojima and H. Yoshioka for their assistance in VSM and XPS measurements. This work was partly supported by Grants-in-Aid for Scientific Research Nos. 0621106, 06403021, and 07555271 from Ministry of Education, Science, Sports, and Culture of Japan. Financial supports from The Mazda Foundation, The Research Foundation for Materials Science, and The Hosokawa Powder Technology Foundation are also acknowledged. H.I. is in receipt of a Fellowship from the Japan Society for the Promotion of the Science for Japanese Junior Scientists.

CM970036Z